

Electrochemical behaviour of Mild Steel in Acidic Medium Based on Eco-Friendly Stabilized Monodisperse Silver Nanocomposite

Ayman M. Atta^{1,2}, Gamal A. El-Mahdy^{1,3,*}, Hamad A. Al-Lohedan¹ and Abdelrahman O. Ezzat

¹ Surfactants research chair, Department of Chemistry, College of Science, King Saud University, Riyadh 11451, Kingdom of Saudi Arabia.

² Egyptian Petroleum Research Institute, 1 Ahmad Elzomor St., Nasr city, Cairo, Egypt.

³ Chemistry Department, Faculty of Science, Helwan University, Helwan, Egypt.

*E-mail: gamalmah2000@yahoo.com

Received: 30 August 2014 / *Accepted:* 7 October 2014 / *Published:* 28 October 2014

Among the natural products, plant extracts and gums find a prominent place. The abundant phytochemical constituents of plant extracts and gums possess considerable potential as inexpensive, non-toxic and renewable sources of a wide range of organic chemicals of industrial significance. The present work used Myrrh gum to prepare monodisperse coated silver nanoparticles. The method used is simple, easy, cost effective and environment friendly. In this study, Myrrh was used for the first time as a reducing and stabilizing agent. X-ray diffraction, ultraviolet visible spectra, transmission electron microscopy, and ultrasonic spectroscopy revealed the formation of monodispersed Ag-NPs with a narrow particle size distribution. The electrochemical behaviour of Myrrh and silver nanoparticles on steel in 1 M HCl solution has been studied by potentiodynamic and EIS measurements. The inhibition efficiency increases with the concentration of Myrrh and silver nanoparticles. The results revealed that inhibitive effect of silver nanoparticles with Myrrh significantly improved the inhibition performance, and produced strong synergistic inhibition effect.

Keywords: Silver nanoparticles; Myrrh, electrochemical, steel, polarization, EIS

1. INTRODUCTION

The study of corrosion inhibition of mild steel using green inhibitor in acidic media, containing HCl in particular, is one of the challenging topic of current research in various industries involving chemical cleaning, descaling, pickling, acid oil-well acidizing, etc. [1-3]. A new generation of corrosion inhibitors based on dispersed nanoparticles and nanocomposites can be used as dispersed

phase or in smart organic coatings for steel [4-6]. These materials named as nanocontainers that can respond quickly to changes in the corrosive environment. The electrochemical behavior of corrosion inhibitors encapsulated within nanocontainers was triggered by the corrosion process to inhibit these environments [7-9]. Moreover, these materials have superior properties such as antibacterial, anticorrosion and antistatic. One of the disadvantages of these materials is the direct introduction of inhibitor components into protective coatings very often which leads to the degradation and deactivation of a corrosion inhibitor and of the polymer matrix [10]. To overcome this limitation, the complexation of organic molecules by cyclodextrin [11] or the use of oxide nanoparticles, which can play the role of nanocarriers for corrosion inhibitors adsorbed on their surface. The design of these materials is based on the core-shell structure in which the nanocontainers should have good compatibility with the matrix components. Moreover, a shell should have permeability properties that can be controlled by external stimuli.

Silver nanoparticles, Ag NPs, have attracted tremendous attentions due to their favored biological activity, thermal, optical and electrical properties [12-14]. There are several methods [15-17] have been used to prepare Ag NPs based on reduction of silver nitrate using hazardous chemicals such as organic solvents, reducing agent, and stabilizing agent. Several attempts were used to prepare Ag NPs based on bio-materials and electrochemical methods [18-20]. The low yield and stability of Ag NPs to the environmental conditions such as sun light, chemical reagents, pH were the major disadvantages of these methods. Moreover, increment the toxicity of Ag NPs due to slow dissolution under release of silver ions at the storage still unsolved problem. There are several challenges to prepare Ag NPs such as monodispersity, size and shape control, reproducibility, scale up, building complex nanostructures and reduction the preparation cost. The aim of the present work was to develop a new, simpler, economically feasible method to prepare mono-dispersed and stabilized silver nanoparticles at low temperature to facilitate their applications. In this respect, Myrrh is considered as an alternative biopolymer for the coating and stabilization of nanostructures, including iron oxide magnetic nanoparticles (MNPs) [21]. This paper describes the effect of Myrrh on the synthesis of AgNPs, using an easy green chemistry method. In this work, we have used Myrrh to cap the surface of silver nanoparticles (Ag NPs), by an adsorption mechanism. It is postulated that the amide, hydroxyl or carboxylate groups in Myrrh are responsible for its adsorption on the surface of Ag NPs. The application of the prepared Ag NPs as green corrosion inhibitors for steel was investigated using different electrochemical methods.

2. EXPERIMENTAL

2.1. Materials

Myrrh gum produced from a spiny deciduous thorny tree or shrub which grows as thickets to the height of 15 feet in Saudi Arabia desert regions. The soluble fraction of Myrrh was extracted from ethanol/water (1:1 volume %) and used as capping agent after recovery using a vacuum evaporator. Silver nitrate, poly (vinyl pyrrolidone) having molecular weight 40000 g/mol (PVP), ammonia solution 25 % and sodium hydroxide purchased from Aldrich Sigma Co. were all used without purification. The

steel with the chemical composition (wt%) 0.14% C, 0.57% Mn, 0.21% P, 0.15% S, 0.37% Si, 0.06% V, 0.03% Ni, 0.03% Cr and Fe balance was used in this study as working electrode(WE). Prior to all measurements, the samples were abraded with emery paper from 400 grit to 4000, degreased ultrasonically in ethanol, and dried at room temperature.

2.2. Preparation of Ag NPs

2.2.1. Preparation of Ag/PVP NPs:

PVP-coated silver nanoparticles were prepared by reduction of silver nitrate (AgNO_3) in the presence of both glucose and PVP according to Wang et al.[22]. Briefly, 2 g of glucose and 1 g of PVP were dissolved in 40 g of water and heated to 90 °C. Then, 0.5 g of AgNO_3 dissolved in 1 mL of water was quickly added. The dispersion was kept at 90 °C for 1 h until the color changed to be brown and then cooled to room temperature. The particles were collected by ultracentrifugation (30 000 rpm; 30 min), redispersed in pure water and collected again by ultracentrifugation. The typical yield with respect to Ag was about 5%.

2.2.2. Synthesis of coated Ag/ Myrrh NPs:

Myrrh coated silver nanoparticles were synthesized as the same reported procedure used for preparation of Ag/PVP NPs but Myrrh 2 g was replaced both PVP and glucose and 50 ml of ammonia solution (25 Wt %) was added to the reaction mixture. The reaction temperature was kept until the color changed from yellow to brown. The yield of reaction was 65 % after collecting the particles with ultracentrifuge and washing with water and ethanol several times.

2.3. Characterization of Ag NPs

X-ray powder diffraction (XRD) patterns were recorded using a D/max 2550 V X-ray diffractometer (X'Pert, Philips, Eindhoven, Netherlands). Transmission electron microscopy (TEM) micrographs were taken with a JEOL JEM-2100F (JEOL, Tokyo, Japan). A few drops of silver nanoparticle solution were diluted into 1 mL of ethanol, and the resulting ethanol solution was placed onto a carbon coated copper grid and allowed to evaporate. HR-TEM images of the nanocomposites were recorded using a JEM-2100F (JEOL) at an acceleration voltage of 200 kV.

The Ultrasizer ultrasonic spectrometer (Malvern Instruments, Worcestershire, U.K.) can measure sound attenuation and sound velocity as a function of frequency, giving particle size distributions of Ag NPs.

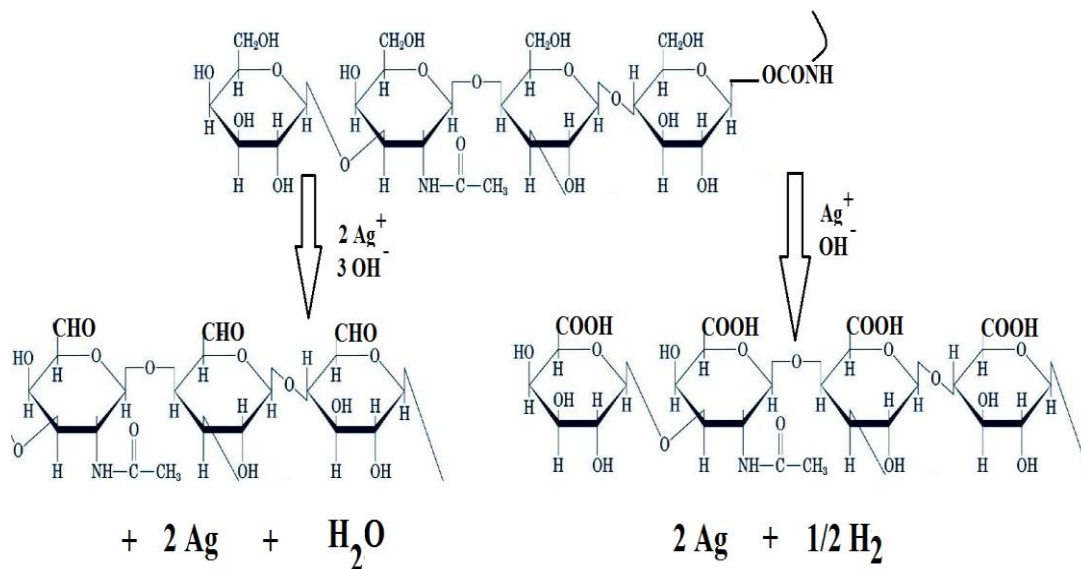
Ultraviolet-visible (UV-Vis) absorption spectra were obtained with a Techcomp UV2300 spectrophotometer ((Shanghai, China). Different concentrations of aqueous solutions of HCl (1 M) were used to evaluate the stability of the synthesized Ag NPs.

2.4 Electrochemical measurements

Electrochemical experiments were carried out in a conventional three-electrode cell with a platinum sheet as counter electrode (CE) and a saturated calomel electrode (SCE) as the reference electrode (RE). Measurements were performed using the Solartron 1470E (multichannel system) as electrochemical interface and the Solartron 1455A as Frequency response analyzer. Data were collected and analysed using CorrView, CorrWare, Zplot and ZView software, developed by Scribner Associates, Inc. The potentiodynamic current potential curves were recorded with a scanning rate of 1 mV/s. EIS measurement was carried out within the 10 kHz–1 mHz frequency range with an amplitude of 10 mV.

3. RESULTS AND DISCUSSION

Among the various chemical methods reported for production of Ag NPs, many reducing agents had been attempted, including formaldehyde, hydrazine, glucose, ascorbic acid, ferric ion, ethylene glycol [23-27], etc. Chemical reduction of transition metal precursor salts, in the presence of chemical stabilizing and reducing agents, is one of the most common methods for the preparation of nanoparticles.



Scheme 1

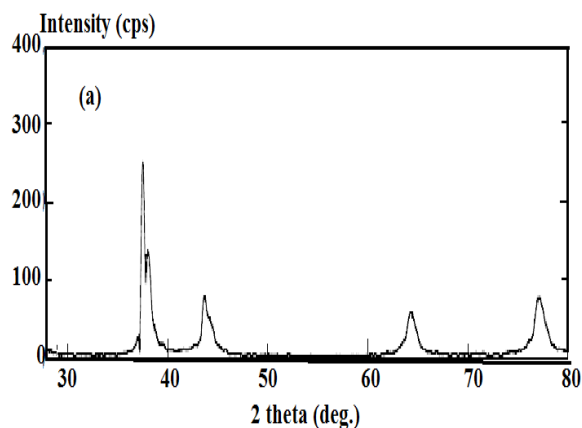
Furthermore, the synthesis of Ag NPs in a colloidal solution requires the use of methods to obtain a precise control, on nanoparticle size and shape. These methods have achieved a set of monodisperse particles, with a very specific particular property. There is no any report used Myrrh as capping agent to produce Ag NPs. Also, the reduction reaction of metallic ions is sensitive to the pH of the reduction solutions. Moreover, it may also affect the morphology of nanoparticles. It was reported that [28] increase of pH led to a decrease of aspect ratio of silver nanorods and an increase of

monodispersity. It had been mentioned by many researchers that the addition of alkaline ion is necessary to carry out the reduction reaction of metallic ions. The present work aims to use Myrrh as reducing and capping agent in the presence of alkaline solution. The chemical structure of water soluble fractions (70% of Myrrh) was previously reported [29]. The chemical structure was based on polysaccharides and polyglycoprotein. The reduction of silver nitrate by Myrrh gum in the presence of hydroxyl ions can be illustrated in Scheme 1.

The scheme 1 shows that with a greater amount of hydroxyl ions (increased pH value), the reduction reaction is favored since the partial processes take place with a higher yield. It is well known that when AgNO_3 was mixed with NaOH only, one obtained pure Ag_2O precipitate. However, if a reducing reagent was also added, the product became pure Ag [30]. This fact implied that the transformation from Ag_2O to Ag was very fast within these reaction systems [31]. The method for preparing AgNPs using Myrrh as a protective agent in water is quite simple, but no reports have been found describing the effect of the size of the Myrrh as a stabilizing agent on the synthesis of AgNPs in an aqueous solution at room temperature. The most accepted mechanism for the formation of nanoparticles, including their growth, considers the type of the stabilizing agent used, which influences the shape and size of the nanoparticles (Scheme 1). It was expected that this method has the advantage of reproducibility and capacity to obtain monodisperse colloids, with a narrow distribution in particle size.

3.1. Characterization of the prepared Ag NPs

The X-ray powder diffraction (XRD) can be used to confirm the formation of AgNPs either in the presence of PVP or Myrrh as capping and reducing agents. In this respect, XRD patterns of the prepared AgNPs were represented in Figure 1a and b. It was observed that Ag NPs coated with PVP and Myrrh have similar diffraction profiles. The XRD peaks at 2θ of 35.9° , 42.1° , 62.8° , 75.7° and 82.7° can be attributed to the (111), (200), (220), (311) and (222) crystallographic planes of face-centered cubic (fcc) silver crystals, respectively (Ref. # 01-087-0597). It was confirmed that, the main crystalline phase was silver; no obvious impurities (e.g., Ag_2O [32]).



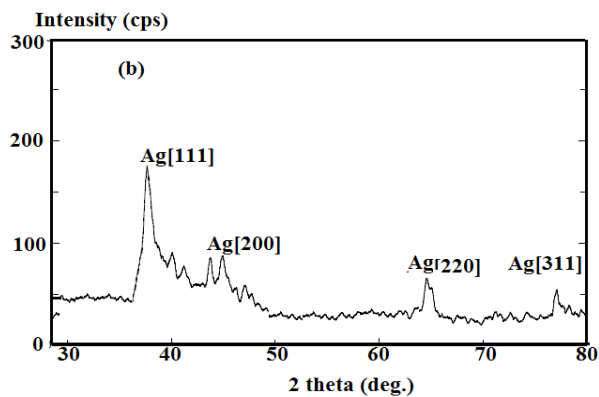


Figure 1. XRD patterns of AgNPs coated with a)PVP and b)Myrrh.

Moreover, no other peaks related to an impurity, indicating that the silver metal was relatively pure. It was also proved that the broadness of the XRD peaks indicates the nanocrystalline nature of Ag nanoparticles.

TEM analyses show the effect of the Myrrh on the shape, size and dispersity of AgNPs obtained and also used to confirm the capping of the metal nanoparticles with polymers or capping agents. The TEM micrographs of the prepared Ag NPs were illustrated in Figure 2a and b. The TEM images demonstrate that the AgNPs obtained in the presence of PVP (Figure 2a) spherical in shape with possibility to grow into larger aggregates.

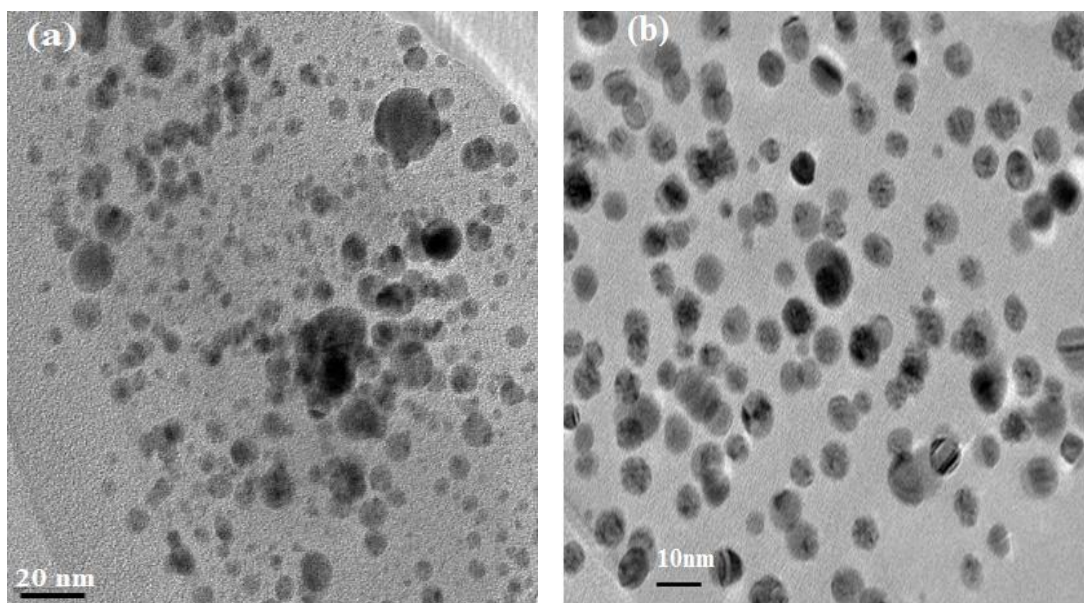


Figure 2. TEM micrographs of AgNPs coated with a)PVP and b)Myrrh.

The Ag NPs coated with PVP (figure 2a) shows polydispersity and broad particle size ranged from 5 to 23 nm. The TEM results indicated that the obtained Ag NPs coated with Myrrh (figure 2b) have a smaller size and narrower size dispersity and the average size of all prepared Ag-NPs was

ranged from 9 to 12 nm. The core-shell structure was confirmed from Figure 2 which reveals that the Ag NPs appeared as black core while PVP or Myrrh appeared as transparent shell. This was attributed to the silver nanoparticles can absorb the electron beam. The TEM results indicated that Myrrh formed stabilized and monodispersed Ag NPs. It was found that the particle size of Ag-NPs obtained in Myrrh solutions is smaller than in the PVP-glucose solutions, which can be related to rate of reduction reaction [33].

The particle size of Ag NPs and their distribution can be analyzed using ultrasizer. The data of particle size of Ag NPs coated with PVP and Myrrh was illustrated in Figure 3 a, and b, respectively. Figure 3 show that, the particle size distribution of Ag/PVP is polydisperse and greater particle size ranged from 3 to 25 nm. Ag NPs capped with Myrrh monodisperse and the particle size was ranged from 9.3 to 12.5 nm. These data indicated that the Myrrh was good reducing and capping agents to produce core-shell Ag NPs. These results demonstrated good agreement with the results obtained in the transmission electron microscopy (TEM) images of Ag-NPs and their particle size distribution. From the above mentioned we can conclude that the Myrrh is the best stabilizing agent, because these particles have a smaller size and narrower size distribution.

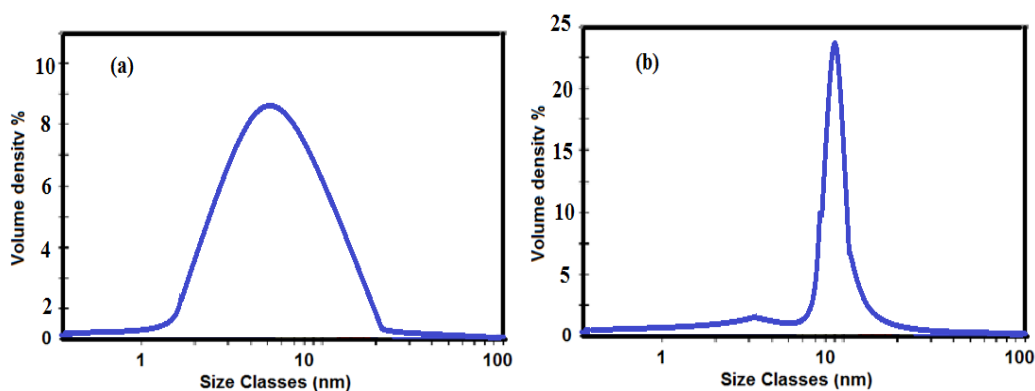


Figure 3. Particle size distribution of AgNPs coated with a)PVP and b)Myrrh.

3.2. Acid stability of Ag NPs

It is well known that in the nanoscale, chemical and physical properties of inorganic nanoparticles are highly dependent on factors such as size and shape for two different reasons. The first one is that nano-materials have, relatively, a larger surface area for the same mass of similar material, which increases their chemical reactivity. The second one is that, below 50 nm, the laws of classical physics behave differently from those of the same material on a larger scale. It was previously reported that the acid stability of silver towards HCl was decreased when the size of silver converted to nanosize [34]. In previous work, we succeeded to prepare stabilized Ag NPs with capping with modified poly(vinyl alcohol) [35]. The present work will investigate the stability of the Ag NPs towards 1 M HCl using UV- visible analysis. The data were illustrated in Figure 4. The formation of Ag-NPs was studied using UV-vis spectroscopy, which has proven to be a very useful technique for

the analysis of nanoparticle formation over time. The obtained AgNPs displayed absorption peaks, the characteristic surface plasmon resonance (SPR) band for silver, centered from 405 to 427 nm for Ag NPs coated with Myrrh and PVP, respectively. The small shift to the left (blue-shift) or to the right (red-shift) in the λ_{max} of the SPR peak could be related to obtaining Ag-NPs at various shapes, sizes, or solvent dependencies of formed Ag-NPs. This phenomenon indicated that the size of particles was reduced, because the absorbance peak due to the SPR of metallic nanoparticles shows the blue-shift with decreasing particle size [36]. Careful inspection of data, figure 4, showed that Ag NPs coated with Myrrh has high absorption more than that coated with PVP. This observation reveals the high yield conversion of Ag NPs in the presence of Myrrh.

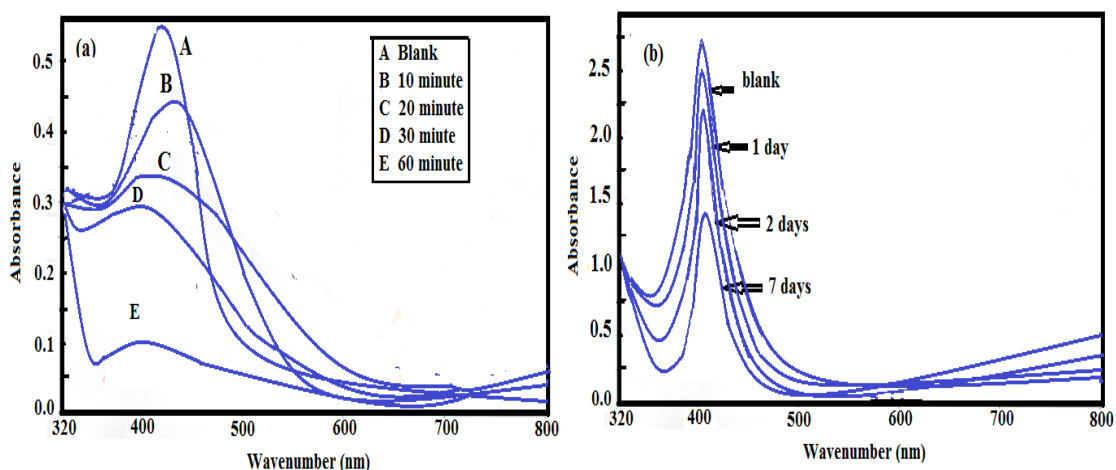


Figure 4. UV- visible spectra of AgNPs coated with a)PVP and b)Myrrh in 1 M HCl for interval times.

As indicated from Figure 4, the broadening of the SPR peak Ag NPs coated with PVP increased with time when compared to the Ag NPs capped with Myrrh. Moreover, the absorbance of peaks decreased with time when Ag NPs coated with PVP immersed in 1 M HCl for 1h. This data indicated the poor stability of Ag NPs coated with PVP towards 1 M HCl due to dissolution of Ag NPs and formation of AgCl [35]. The broadening of peaks was referred to agglomeration of Ag NPs followed by dissolution to form AgCl precipitate. Careful inspection of data, Figure 4 b, indicated that the Ag NPs coated with Myrrh possess high acid stability to 1 M HCl for 1 week without aggregations and dissolution. The high acid stability of Ag NPs coated with Myrrh confirms the ability to use as corrosion inhibitors in 1 M HCl.

3.3. Polarization studies

The polarization behavior of steel in 1.0 M HCL solution in the absence and presence of different concentrations of Ag-Myrrh nanoparticles is shown in Figure 5. The presence of Ag-Myrrh nanoparticles causes a decrease in the corrosion rate i.e. shifts the cathodic and anodic curves to lower current densities. This may be ascribed to adsorption of inhibitor over the active sites and

drastically inhibited both anodic and cathodic reactions. As the concentration of Ag nanoparticles increases, the shift in the cathodic and anodic line increases indicating that the behavior of Ag-Myrrh nanoparticles acts as a mixed type inhibitor.

Table 1. Inhibition efficiency values for steel in 1M HCl with different concentrations of Ag-Myrrh nanoparticles calculated by Polarization and EIS methods.

| Polarization Method | | | | | EIS Method | | | |
|---------------------|---------------|---------------|-------------------|----------------------------|------------|-----------------|---------------------------|--------|
| | B_a (mV) | B_c (mV) | E_{corr} (V) | i_{corr} $\mu A/cm^2$ | $IE\%$ | R_{ct} Ohm | Cdl ($\mu F/cm^2$) | $IE\%$ |
| Blank | 69.00 | 120.00 | -0.3955 | 839 | — | 1.80 | 334 | — |
| 50 ppm | 125.85 | 110.80 | -0.4589 | 236 | 71.87 | 6.2 | 178 | 70.96 |
| 100 | 77.01 | 102.01 | -0.4355 | 166 | 80.00 | 6.6 | 182 | 72.72 |
| 150 | 70.14 | 113.35 | -0.4263 | 132 | 84.26 | 10.9 | 131 | 83.48 |

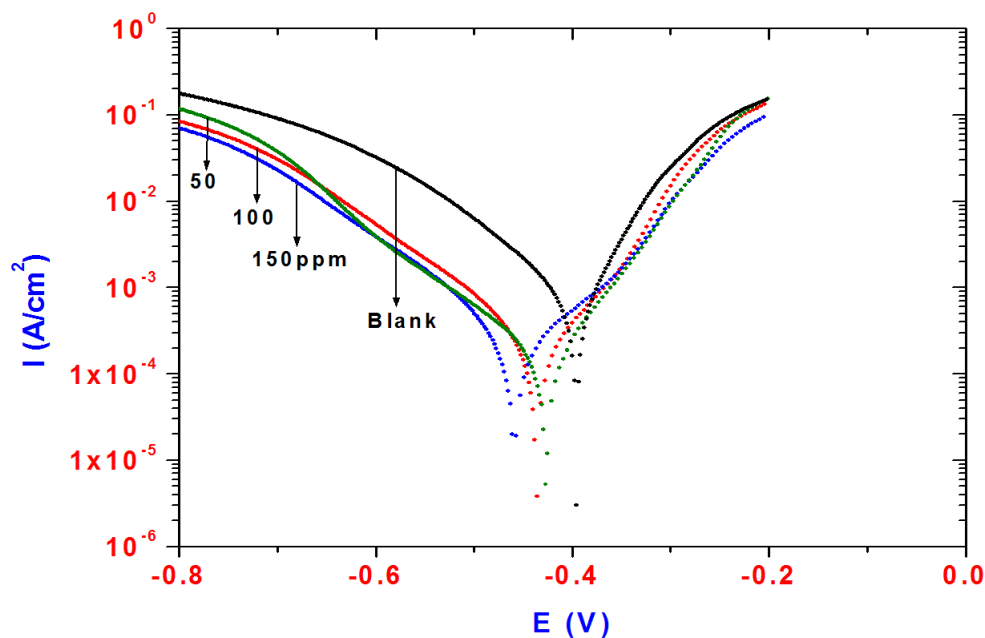


Figure 5. Polarization curves for steel in 1M HCl solution containing Ag-Myrrh nanoparticles with different concentrations.

The results can be explained on the basis that the formed inhibitive film adsorbed on both anodic and cathodic reactive sites, which inhibited the anodic and cathodic reactions of steel corrosion. Upon addition of Myrrh to Ag nanoparticles, the corrosion current decreased remarkably, indicating that the steel corrosion was drastically inhibited. The electrochemical parameters obtained from the

polarization curves, for Ag-Myrrh nanoparticles such as corrosion potential (E_{corr}), cathodic and anodic Tafel slopes (B_a and B_c) and corrosion current density (i_{corr}) obtained by extrapolation of the Tafel are listed in Table 1. The protection efficiency (PE%) is evaluated from i_{corr} values using the relationship [37-38]:

$$\text{PE\%} = 1 - i_{\text{corr (inh)}} / i_{\text{corr}}^0 \times 100 \quad (1)$$

Where $i_{\text{corr (inh)}}$ and i_{corr}^0 corrosion current densities in the presence and absence of inhibitor, respectively. The values of PE% with different inhibitor concentrations of Ag-Myrrh nanoparticles are listed in Table 1.

This result confirms that the presence of Myrrh with Ag nanoparticles had strong inhibitive effect on the electrochemical behavior of steel in 1M HCl. The values of PE% increased with inhibitor concentrations, which indicate that, this mixture act as good inhibitors.

3.4.EIS measurements

Figure 6 shows the Nyquist diagrams for steel in 1 M HCl solution with various concentrations of Ag-Myrrh nanoparticles. It is apparent, from these plots that, the impedance response of steel corrosion in blank solution has significantly changed after the addition of inhibitor. The Nyquist plots reveal that each impedance diagram consists of a capacitive loop and its diameter increases with the increase of inhibitor concentration. The single capacitive loop can be attributed to the charge transfer that takes place at steel/solution interface, and the transfer process controls the electrochemical reaction of steel. The equivalent circuit employed for fitting the experimental data composed of a solution resistance (R_s) in series with the parallel combination of the charge transfer resistance (R_{ct}) and the double layer capacitance (C_{dl}). The impedance parameters for Ag-Myrrh nanoparticles obtained by fitting the EIS data to the equivalent circuit are listed in Table 1. It can be observed that the values of R_{ct} increase while the values of C_{dl} decrease with increase in concentration of Myrrh + Ag nanoparticles. The decrease in C_{dl} on adding Ag-Myrrh nanoparticles to the acid solution indicates the presence of a protective layer that covers the surface of the electrode. The adsorption of Ag-Myrrh nanoparticles on the steel surface decreases C_{dl} because they displaced the water molecules and other ions that were originally adsorbed on the surface. The thickness of the protective and inhibitive layer or the surface coverage by Ag-Myrrh nanoparticles increased due to more adsorption of Ag-Myrrh nanoparticles on the steel surface [39]. It can be observed that the addition of Ag nanoparticles to acid solution containing Myrrh is accompanied by further enhancing of R_{ct} values and reducing C_{dl} values. In accordance, the inhibition efficiencies increase markedly in the presence of Ag nanoparticles. The protection efficiency (PE%) was calculated from the charge transfer resistance (R_{ct}) using the following formula:

$$\text{PE\%} = 1 - R_{ct}^1 / R_{ct}^2 \times 100 \quad (2)$$

Where R_{ct}^1 , and R_{ct}^2 were referred the charge transfer resistances in absence and presence of the inhibitors, respectively. The values of PE% at different inhibitor concentrations are given in Table 1. The higher value of PE% with the addition of silver nanoparticles to Myrrh can be accounted to an increase in the adsorption tendency of the inhibitor mixture on the steel surface with a formation of

dense and tight protective film, which drastically decreases the steel surface corrosion. This behavior can be attributed to the synergistic effect of Myrrh and Ag nanoparticles. It can be concluded that the addition of silver nanoparticles could play a principal role in enhancement of performance of an eco-friendly Myrrh film adsorbed on the steel substrate. The inhibition efficiencies calculated from EIS are in good agreement with those obtained from potentiodynamic polarization.

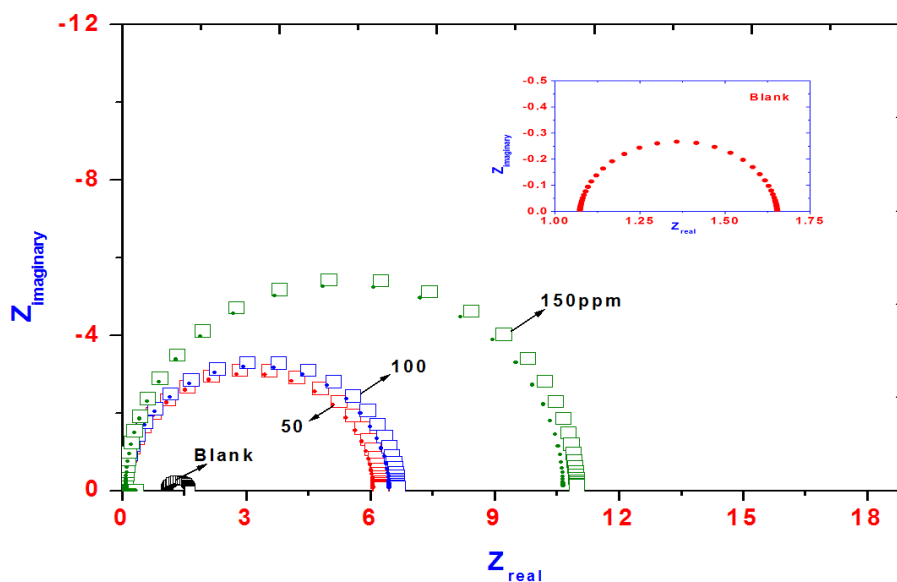


Figure 6. Nyquist diagram for steel in 1 M HCl solution containing Ag-Myrrh nanoparticles with different concentrations showing experimental (square) and fitted data (circle).

4. CONCLUSION

1. A novel method has been developed for the preparation of Ag NPs, using Myrrh as the reducing and stabilizing agents.
2. Ag NP suspensions were prepared that were stable in 1 M HCl more than one week. Indicated that monodispersity and formation of stable core-shell Ag-Myrrh nanoparticle.
3. The method can be successfully used in ecological processes for the preparation of Ag NPs.
4. Electrochemical measurements revealed that incorporation of silver nanoparticles with Myrrh significantly improved the inhibition performance, and produced strong synergistic inhibition effect.
5. All EIS spectra exhibit one capacitive loop which indicates that the electrochemical reaction is controlled by charge transfer process.
6. The addition of silver nanoparticles to Myrrh solution behaves as a mixed-type inhibitor, which inhibits both anodic and cathodic reactions.
7. The electrochemical measurements indicated that stabilized monodisperse silver Nanoparticles can be used as corrosion inhibitor for steel in 1 M HCl.

ACKNOWLEDGEMENT

The project was supported by King Saud University, Deanship of Scientific Research, Research Chair.

References

1. P. Mourya, S. Banerjee, M.M. Singh, *Corrosion Science*, 85 (2014) 352.
2. W. Meier, *Chem. Soc. Rev.* (2000) 29, 295
3. X. Lu, Z. Xin, *Colloid Polym. Sci.*, 284 (2006) 1062
4. D.Shchukin, H.Möhwald, *Adv. Funct. Mater.*, 17(2007) 1451.
5. A.M. Atta, G. A. El-Mahdy, H. A. Al-Lohedan, A. O. Ezzat, *Molecules* 19(2014) 6246-6262
6. N. Selvakumar, K. Jeyasubramanian, R. Sharmila, *Progress in Organic Coatings*, 74 (2012) 461-469.
7. G. Schneider, G. Decher, *Nano Lett.* 4 (2004) 1833
8. D.V. Andreeva, D. Fix, H. Möhwald, D.G. Shchukin, *J. Mater. Chem.* 18(2008) 1738.
9. D. Shchukin, H. Möhwald, *Adv. Funct. Mater.*, 17(2007) 1451.
10. D. G. Shchukin, M. Zheludkevich, K. Yasakau, S. Lamaka, M. G. S. Ferreira, H. Möhwald, *Adv. Mat.* (2006) 18, 1672
11. B. Leggat, W. Zhang, R. G. Buchheit, S. R. Taylor, *Corrosion*, 58 (2002) 322.
12. A. Sutton, G. Franc, A. Kakkar, *J. Polym. Sci. Polym. Chem.* 47 (2009) 4482–4493.
13. I.N. Ghosh, S.D.Patil, T. K. Sharma, S.K.Srivastava, R. Pathania, N. K. Navani, *International Journal of Nanomedicine*, 8 (2013)4721–4731.
14. M. F. Ottaviani, R. Valluzzi and L. Balogh, *Macromolecules*, 35(2002) 5105.
15. Y. Yin, Z-Y. Li, Z. Zhong, B. Gates, Y. Xia, S. Venkateswaran, *J. Mater. Chem.*, 12 (2002) 522–527.
16. M. Yamamoto, M. Nakamoto, *J. Mater. Chem.*, 13 (2003) 2064–2065.
17. S. Kittler, C. Greulich, J. Diendorf, M. Koller, M. Eppele, *Chem. Mater.*, 22 (2010) 4548–4554.
18. R. A. Salkar, P. Jeevanandam, S. T. Aruna, Yuri Koltypin and A. Gedanken, *J. Mater. Chem.*, 9 (1999)1333–1335.
19. L. Sintubin, W. Verstraete, N. Boon, *Biotechnology and Bioengineering*, 109 (2012) 2422.
20. L. Rodri'guez-Sa'nchez, M. C. Blanco, M. A. Lo'pez-Quintela, *J. Phys. Chem. B*, 104 (2000) 9683-9688.
21. A. M. Atta, H,d A. Al-Lohedan, S. A. Al-Hussain, *Molecules*, 19 (2014) 11263-11278.
22. H.Wang, X.Qiao, J. Chen, S. Ding, *Colloids Surf., A*, 256 (2005)111.
23. K.S. Chou, Y.S. Lai, *Mater. Chem. Phys.*, 83 (2004) 82–88.
24. S.P. Wu, S.Y. Meng, *Mater. Chem. Phys.*, 89 (2005) 423–427.
25. I. Sondi, D.V. Goia, E. Matijevic, *J. Colloid Interface Sci.*, 260 (2003)75.
26. G.D. Wei, Y. Deng, C.W. Nan, *Chem. Phys. Lett.* 367 (2003) 512.
27. P.V. Silvert, R. Herrera-Urbina, N. Duvauchelle, V. Vijayakrishnan, K.T. Elhsissen, *J. Phys. Chem.* 6 (1996) 573–577.
28. G.J. Lee, S.I. Shin, Y.C. Kim, S.G. Oh, *Mater. Chem. Phys.*, 84 (2004) 197–204.
29. L. O. Hanuš, T. Řezanka, V. M. Dembitsky, A. Moussaieff, *Biomed. Papers* 149(1), 3–28 (2005)
30. Z.Y. Huang, G. Mills, B. Hajek, *J. Phys. Chem.* 97 (1993) 11550.
31. K-S. Chou, Y-C. Lu, H-H. Lee, *Materials Chemistry and Physics* 94 (2005) 429–433.
32. P. Raveendran, J. Fu, S.L. Wallen, *J. Am. Chem. Soc.*, 125(2003) 13940.
33. M. Darroudi, M. Bin Ahmad, A. Abdullah, N.A. Ibrahim, *International Journal of Nanomedicine*, 6 (2011)569.
34. L. Li, Y-J. Zhu, *Journal of Colloid and Interface Science*, 303 (2006) 415–418
35. A. M. Atta, H. A. Al-Lohedan, A.O. Ezzat, *Molecules*, 19 (2014) 6737-6753.
36. J.R.Heath, *Phys Rev B.*, 40 (1989)9982.

37. E. McCafferty, , *Corros. Sci.* 47 (2005) 3202.
38. Q. Qu, L. Li, W. Bai, S. Jiang, Z. Ding, , *Corros. Sci.* 51 (2009) 2423.
39. J. Zhao, G. Chen, *Electrochim. Acta* 69 (2012) 247.

© 2014 The Authors. Published by ESG (www.electrochemsci.org). This article is an open access article distributed under the terms and conditions of the Creative Commons Attribution license (<http://creativecommons.org/licenses/by/4.0/>).